

*ARMY RESEARCH LABORATORY*



## **Final Report for M-12-08: Rotorcraft Autorotation Study**

**by Andrew Drysdale, Matthew Floros, and Ed Sieveka**

**ARL-TR-6804**

**February 2014**

## **NOTICES**

### **Disclaimers**

The findings in this report are not to be construed as an official Department of the Army position unless so designated by other authorized documents.

Citation of manufacturer's or trade names does not constitute an official endorsement or approval of the use thereof.

Destroy this report when it is no longer needed. Do not return it to the originator.

# **Army Research Laboratory**

Aberdeen Proving Ground, MD 21005-5068

---

---

**ARL-TR-6804**

**February 2014**

---

## **Final Report for M-12-08: Rotorcraft Autorotation Study**

**Andrew Drysdale**

**Survivability/Lethality Analysis Directorate, ARL**

**Matthew Floros**

**Vehicle Technology Directorate**

**Ed Sieveka**

**NAVAIR**

REPORT DOCUMENTATION PAGE			Form Approved OMB No. 0704-0188		
Public reporting burden for this collection of information is estimated to average 1 hour per response, including the time for reviewing instructions, searching existing data sources, gathering and maintaining the data needed, and completing and reviewing the collection information. Send comments regarding this burden estimate or any other aspect of this collection of information, including suggestions for reducing the burden, to Department of Defense, Washington Headquarters Services, Directorate for Information Operations and Reports (0704-0188), 1215 Jefferson Davis Highway, Suite 1204, Arlington, VA 22202-4302. Respondents should be aware that notwithstanding any other provision of law, no person shall be subject to any penalty for failing to comply with a collection of information if it does not display a currently valid OMB control number. <b>PLEASE DO NOT RETURN YOUR FORM TO THE ABOVE ADDRESS.</b>					
1. REPORT DATE (DD-MM-YYYY) February 2014		2. REPORT TYPE Final		3. DATES COVERED (From - To) October 2011–September 2013	
4. TITLE AND SUBTITLE  Final Report for M-12-08: Rotorcraft Autorotation Study			5a. CONTRACT NUMBER		
			5b. GRANT NUMBER		
			5c. PROGRAM ELEMENT NUMBER		
6. AUTHOR(S) Andrew Drysdale, Matthew Floros, and Ed Sieveka *			5d. PROJECT NUMBER M-12-08		
			5e. TASK NUMBER		
			5f. WORK UNIT NUMBER		
7. PERFORMING ORGANIZATION NAME(S) AND ADDRESS(ES) U.S. Army Research Laboratory ATTN: RDRL-SLB-D Aberdeen Proving Ground, MD 21005-5068			8. PERFORMING ORGANIZATION REPORT NUMBER ARL-TR-6804		
9. SPONSORING/MONITORING AGENCY NAME(S) AND ADDRESS(ES) Joint Aircraft Survivability Program Office 735 S. Courthouse Road Suite 1100 Arlington, VA 22204-2489			10. SPONSOR/MONITOR'S ACRONYM(S) JASPO		
			11. SPONSOR/MONITOR'S REPORT NUMBER(S)		
12. DISTRIBUTION/AVAILABILITY STATEMENT Approved for public release; distribution is unlimited.					
13. SUPPLEMENTARY NOTES * Naval Air Warfare Center Aircraft Division, 48110 Shaw Rd., Unit 5, Patuxent River, MD 20670-1906					
14. ABSTRACT A system for automated execution of the DESCENT rotorcraft autorotation model was developed, and a sensitivity study of various input parameters was completed for an analysis involving a generic air vehicle. Separately, the structural dynamics of an impacting helicopter were modeled in the MADYMO structural dynamics model to better inform the optimization priorities of DESCENT. The structural modeling explored loading transmitted to hypothetical occupants as well as vehicle loading.					
15. SUBJECT TERMS rotorcraft, autorotation, DESCENT, JASPO, survivability					
16. SECURITY CLASSIFICATION OF:			17. LIMITATION OF ABSTRACT	18. NUMBER OF PAGES	19a. NAME OF RESPONSIBLE PERSON Andrew Drysdale
a. REPORT Unclassified	b. ABSTRACT Unclassified	c. THIS PAGE Unclassified	UU	32	19b. TELEPHONE NUMBER (Include area code) (410) 278-4762

---

## Contents

---

<b>List of Figures</b>	<b>iv</b>
<b>List of Tables</b>	<b>v</b>
<b>1. Introduction</b>	<b>1</b>
<b>2. Objective Function Parameterization</b>	<b>1</b>
2.1 Motivation: Intelligently Tailored Maneuvers .....	2
2.2 Description of Work Done .....	2
2.2.1 DESCENT Improvements .....	2
2.2.2 Code Execution Automation .....	5
2.2.3 Parametric Analyses .....	5
2.3 Results .....	7
2.3.1 Study 1: Gross Weight/Pilot Delay/Velocity Components .....	7
2.3.2 Study 2: Fuselage Pitch Target and Weighting .....	9
2.3.3 Study 3: Max $C_T$ Rate of Change/Max $\alpha$ Rate of Change/Gross Weight .....	10
2.3.4 Study 4: In-Maneuver Vertical Speed Weighting and Target/Gross Weight .....	11
2.3.5 Study 5: Number of Timesteps/Ambient Air Density/Gross Weight .....	12
<b>3. Out-of-Plane Impact Analysis</b>	<b>15</b>
3.1 Motivation: Intelligent Tradeoffs and Penalties .....	15
3.2 Description of Work Done .....	15
3.2.1 Structural Model Improvement .....	15
3.2.2 Pitch and Roll Study .....	16
3.3 Results .....	17
3.3.1 Loading Time Histories .....	18
3.3.2 Peak Magnitudes .....	21
<b>4. Conclusions</b>	<b>23</b>
<b>Distribution List</b>	<b>24</b>

---

## List of Figures

---

Figure 1. Oscillation of under-damped controls and smoothness term value.....	3
Figure 2. Time-variable weighting function used for rotor speed term. ....	4
Figure 3. $P_k$ vs. maximum thrust rate of change ( $ctsigdotmax$ ) and maximum pitch rate of change ( $alphadotmax$ ).....	7
Figure 4. $P_k$ vs. gross weight and pilot delay for $W_x = 0$ .....	8
Figure 5. $P_k$ vs. gross weight and pilot delay for $W_x = 2.0$ . ....	8
Figure 6. $P_k$ vs. horizontal velocity weighting and pilot delay for $GW = 17,000$ lb.....	9
Figure 7. $P_k$ vs. pitch orientation weighting and target value for $W_x = 2.0$ .....	10
Figure 8. $P_k$ vs. maximum rates for thrust coefficient and angle of attack. ....	11
Figure 9. $P_k$ vs. sink-rate weighting and target value. ....	12
Figure 10. $P_k$ vs. number of time steps and air density for $GW = 15,000$ lb. ....	13
Figure 11. $P_k$ vs. number of time steps and air density for $GW = 18,000$ lb. ....	13
Figure 12. Horizontal (blue) and vertical (red) impact velocities vs. number of time steps. ....	14
Figure 13. Execution time vs. number of time steps.....	15
Figure 14. Example of mesh improvement in Bell-206-based structural model. ....	16
Figure 15. Helicopter model impacting vertically at $10^\circ$ (nose-down) pitch and $10^\circ$ (port) roll.....	17
Figure 16. Copilot neck moments for $10^\circ$ (nose-down) pitch impacts. Roll conditions are flat (green), $2^\circ$ (blue), $5^\circ$ (red), and $10^\circ$ (yellow).....	17
Figure 17. Copilot y-axis lumbar loads for vertical impact and flat landing. In each figure, green, blue, red, and yellow traces represent $0^\circ$ , $2^\circ$ , $5^\circ$ , and $10^\circ$ of fuselage roll, respectively. ....	18
Figure 18. Copilot z-axis lumbar loads for vertical impact and flat landing. ....	19
Figure 19. Copilot x-axis (left) and y-axis (right) lumbar loads for vertical impact and nose-up landing.....	19
Figure 20. Copilot x-axis (left) and y-axis (right) lumbar loads for vertical impact and nose-down landing.....	20
Figure 21. Pilot x-axis (left) and z-axis (right) neck moments for vertical impact and nose-up landing.....	20
Figure 22. Pilot z-axis pelvic acceleration (g) vs. pitch and roll impact state. ....	21
Figure 23. Pilot z-axis pelvic acceleration (g) vs. pitch and roll impact state. ....	22
Figure 24. Pilot y-axis pelvic acceleration (g) vs. pitch and roll impact state. ....	22

---

## List of Tables

---

Table 1. Objective function terms and explanation. ....	4
---	---

INTENTIONALLY LEFT BLANK.



---

## 1. Introduction

---

The purpose of this fiscal year 2012–2013 project was to study how different piloting techniques during a helicopter autorotation affect the vehicle’s impact conditions, and how these conditions lead to different predictions of occupant loading and injury. Piloting technique was represented by various parameters in the U.S. Army Research Laboratory DESCENT rotorcraft flight optimization model; varying the parameter values is analogous to changing the priority a pilot puts on the relevant aspect of the maneuver. DESCENT output (impact conditions) was then analyzed for significant trends relating to parameter valuation choices. To model occupant loading, the MADYMO structural dynamics model was used with a helicopter geometry based on the OH-58 Kiowa armed reconnaissance helicopter. The plausible range of DESCENT output was used to create impact scenarios in MADYMO so that different models of pilot decision making might be linked all the way forward to differing occupant injury outcomes.

Parametric studies of pilot prioritization variables (section 2) and impact-state variables (section 3) proceeded along largely independent tracks during the course of the project and are thus presented here independently. Also presented is the background work required to update the relevant models before the studies could begin.

---

## 2. Objective Function Parameterization

---

The DESCENT model iteratively optimizes a helicopter’s autorotation flight path by evaluating the current solution (i.e., the previous flight path computed by DESCENT) via an expression called the objective function. This objective function evaluates to a scalar but can be arbitrarily complex, reflecting as many aspects of the maneuver as desired. DESCENT previously used a function that was limited to the vertical and horizontal impact velocities and a weighting term,  $W_x$ , which defined the relative priority of the horizontal impact velocity in terms of the vertical. This simplified objective function evaluated only the “bottom line” of autorotation—how “hard” the vehicle hit the ground.

For this project, the objective function was broadened to consider several other aspects of the autorotation, listed in detail in section 2.2.1, so that the impact state was more completely described and some basic aspects of piloting technique could be evaluated. Other input quantities that seemed likely to influence the analysis (such as certain vehicle characteristics) were also identified within the input definition. Varying the weightings of these new objective function terms and the values of the input quantities parametrically formed a study of where autorotation outcome was sensitive to these quantities and what the optimal values might be for a set of typical analysis conditions.

## 2.1 Motivation: Intelligently Tailored Maneuvers

DESCENT, as currently constituted, optimizes an autorotation maneuver only with respect to the ultimate vertical-impact velocity, seeking to minimize the velocity. This is a suitable metric for relating the possibility of avoiding structural damage, but on occasion it is desirable to tailor the optimization algorithm to favor a solution with more specific characteristics. For example, certain rotorcraft might have landing gear that makes a high horizontal impact velocity very dangerous (e.g., skids rather than wheels), or conditions of poor visibility might require a more conservative descent velocity than otherwise indicated. The idea behind adding flexibility to DESCENT's objective function is to allow the code to capture additional specific factors to meet the needs of a particular analysis. The ultimate objective is to be able to design maneuvers that correspond to findings (such as those in section 3) concerning which impact states are most optimal for occupant survivability.

## 2.2 Description of Work Done

### 2.2.1 DESCENT Improvements

As described, the DESCENT model's objective function, the expression that scores the quality of the solution, was extensively upgraded to prepare for this project. It expanded from two terms (orthogonal impact velocity components) to seven, including the following:

- Fuselage-pitch orientation at impact
- Fuselage-pitch orientation during flight
- Vertical and horizontal velocity during flight
- Rotor speed during flight
- Control smoothness

Fuselage pitch at impact, and rotor speed and the velocity components during flight, are described in terms of deviation between the current solution and a "target" value. Fuselage pitch during flight is described by the absolute value, from the assumption that a pilot will try to maintain level flight as much as possible during the maneuver. Control smoothness is a generic second-order difference expression, raised to a large exponent to drive small values closer to zero.

$$\left( \frac{\varphi_{i+1} + \varphi_{i-1} - 2\varphi_i}{2 \cdot \Delta\varphi_{max}} \right)^4 \quad (1)$$

This term has the effect of adding to the total value at time steps only where the relevant control level is rapidly toggling between two values as it repeatedly overshoots the "true" value (figure 1). The smoothing term (green series) has a value of 1 when an arbitrary control quantity (blue) oscillates around a setting and a value near zero otherwise. This lets the objective function

identify where oscillation occurs. The optimization algorithm then iteratively minimizes this term's contribution to the overall “score” (objective function valuation) by removing periods of oscillation from the solution.

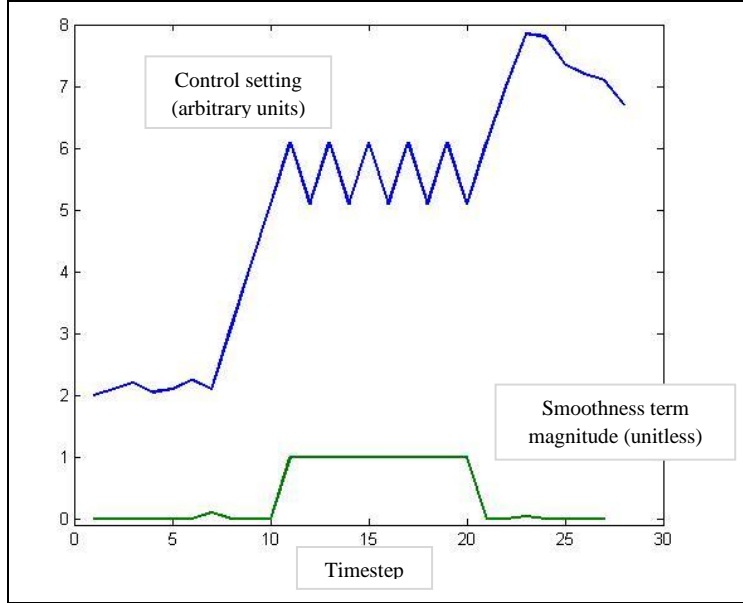


Figure 1. Oscillation of under-damped controls and smoothness term value.

Another improvement was the addition of time-variable weighting expressions. In DESCENT's objective function, each underlying quantity is measured at only the final time step (impact), or at every prior time step, and integrated. In the former case, a global weighting factor is applied to the measurement to prioritize the influence of that quantity relative to other aspects of the maneuver in minimizing the overall objective function. In the latter case, two weighting factors are applied: a global weighting and a time-variable weighting that allows the analysis to prioritize different portions of the maneuver differently. For example, the deviation of the helicopter's rotor speed from the target value (100% of nominal) is weighted with both a global weighting,  $J_\omega$ , and a time-variable weighting expressed as

$$(1 - \varepsilon)\sqrt[4]{x} + \varepsilon x^2 \quad (2)$$

where  $x$  is a function of the dimensionalized time variable  $\varepsilon$ . This expression serves to emphasize rotor speed at the beginning of the maneuver, when thrust is cut (i.e., main rotor collective control setting decreased) to keep the rotor spinning, and ignore the term near the very end of the maneuver (i.e., during the flair to touchdown as collective is increased) when high rotor speed is progressively less critical to maintain (figure 2).

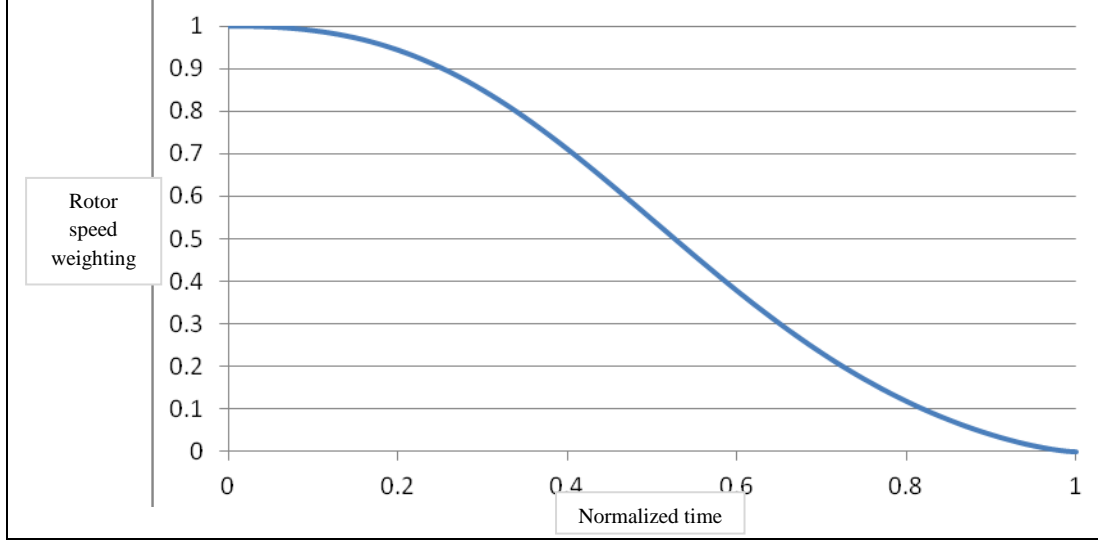


Figure 2. Time-variable weighting function used for rotor speed term.

The full list of objective function terms is shown in table 1. The function takes the form

$$\varphi = v_g + (v_f \text{ weightings})v_f + (\theta_g \text{ weightings})\theta_g + \dots \quad (3)$$

where  $v_g$  is vertical-impact velocity. Vertical-impact velocity is not weighted, so all other weightings are in effect normalized by the emphasis placed on this term.

Table 1. Objective function terms and explanation.

Variable	Quantity	Description/ Notes
$v_f$	Vertical-descent speed	Calculated at each time step as difference between current value and a desired value. Weighted most heavily during “steady descent” middle portion of maneuver.
$v_g$	Vertical-impact speed	Calculated only at impact. Reference against which all other weightings are related.
$u_f$	Horizontal-descent speed	See $v_f$ .
$u_g$	Horizontal-impact speed	Calculated only at impact. Relative weighting is listed as $W_x$ elsewhere in this report.
$\theta_f$	Fuselage pitch	Calculated at each time step as absolute value of fuselage pitch in global coordinates. Weighting increases linearly with proportion of maneuver completed.
$\theta_g$	Fuselage pitch at impact	Calculated only at impact as difference between final value and a desired value.
$\omega_f$	Descending-rotor speed	Calculated at each time step as difference between current value and nominal rotor speed. Weighted most heavily toward beginning of maneuver.
$\Delta f$	Control-level smoothness	Calculated at each time step as second-order difference expression for control quantities. Weighted evenly throughout maneuver.

### 2.2.2 Code Execution Automation

To perform the large number of analyses required for parametric studies in a timely manner, DESCENT was rewritten with case labels to allow for parallel executions, and a script was written to automate the process of executing the model once for each permutation of the relevant parameter values.

The automation script accepts an input file in the Fortran “namelist” format that includes the standard DESCENT input data and one or more concluding lines with the list of values for each varied parameter. It then creates a DESCENT input file with all of the standard data and current values for each of the parameters. This file is named according to which value of each parameter is current, i.e., *uh60\_2\_4\_3* considers the second value of the first parameter, the fourth of the second, and the third of the third. Then the DESCENT executable is called and the analysis is run. The output file is identically named for later storage and processing. When an execution is completed, the script moves to the next permutation of parameters, checks to see if the output file already exists (in which case, a parallel instance is already executing it), and either reruns DESCENT or finds an untaken permutation to run.

### 2.2.3 Parametric Analyses

For this project, five studies were undertaken to assess the effects of different objective function weightings and vehicle characteristic values on the outcome of a DESCENT-modeled autorotation. In general, two aspects of the results were reported: (1) whether impact velocities were significantly sensitive to marginal changes in the parameter values at likely margins for a rotorcraft analysis and (2) whether an optimum parameter value could be discerned for the given conditions. In each case, a “generic” helicopter based on the UH-60 Blackhawk was analyzed.

The problem of how impact velocities would be characterized was somewhat complicated because the autorotation maneuver is very different from different starting points in the helicopter’s flight envelope, so a change in the optimization algorithm might easily have disparate effects depending on the initial conditions. At the same time, it was seen as desirable to express impact velocity changes across the flight envelope in terms of a single metric. This problem was addressed by measuring impact conditions in terms of a “kill probability” ( $P_k$ ). Autorotations were modeled at 80 points in a grid covering the low-speed, low-height portion of the flight envelope; the  $P_k$  is essentially the proportion of those points where the vertical-impact velocity exceeded a specified critical threshold value. A less-optimal set of modeling parameters should cause a rise in impact velocities (more or less) throughout the flight envelope; as more impacts occur at high velocities, the  $P_k$  should increase. By comparing this metric to the  $P_k$ ’s created by other analyses, an approximation can be made of the relative optimality of the current set of parameters. A further advantage of this approach is that the primary application of DESCENT is  $P_k$  production for rotorcraft vulnerability assessments involving engine power loss, so using the metric here ensures that apparent trends in outcome will have some significance in typical use of the model.

The five studies included:

1. Impact horizontal velocity weighting ( $W_x$ ) versus pilot delay period ( $t_d$ ) versus helicopter gross weight ( $GW$ ). Finding “correct” values for  $W_x$  and  $t_d$  has been a matter of some subjective judgment in the past, so investigating how sensitive impact outcomes are to chosen values is worthwhile. Helicopter weight is seen as the primary variable in the overall analysis, so it is included to determine if results differ for light and heavy vehicles.
2. Impact fuselage pitch weighting ( $W_\theta$ ) versus impact fuselage pitch target ( $\theta_l$ ) versus  $W_x$ . This study relates most closely to the occupant-injury analyses discussed in section 3. It is assumed that putting a higher optimization priority ( $W_\theta$ ) on landing with a certain fuselage pitch ( $\theta_l$ ) will have a slightly adverse effect on the impact velocities. Determining how much of an effect will help determine the proper tradeoff between impact orientation and speed in terms of occupant loading. Since the direction of the impact vector (influenced by  $W_x$ ) might play a role, that quantity is also included.
3. Maximum rates of change for rotor pitch and thrust coefficient ( $\alpha$  and  $C_T$ , respectively) versus  $GW$ . These terms—how quickly the control quantities can change—are not well-defined in most real-world analyses. In practice, DESCENT usually uses values that do not significantly inhibit the ability of the optimization algorithm to reach new control levels as required. This study was designed to investigate whether results are sensitive to a wide range of values.
4. In-flight vertical velocity target (*sinkrate*) versus weighting ( $J_{V_z}$ ) versus  $GW$ . A steady-state descent velocity target has not been used before in  $P_k$  production. This study was designed to see if near-optimal impact results are produced when the algorithm is guided toward descending speeds around those measured in flight tests.
5. Number of time steps ( $nt$ ) versus air density ( $\rho$ ) versus  $GW$ . The number of time steps used in the analysis determines the fineness of the state variable integrations through the maneuver. Ambient air density is mainly a function of the air’s pressure and temperature; determining how the  $P_k$  output varies with  $\rho$  (calculated for the altitude at  $t = 0$ ) will determine how applicable results acquired from certain sets of environmental conditions would be to other analyses.  $GW$  is varied to see to what extent the sensitivity of the other two variables depends on the relative “ease” of the autorotation.

Results were visualized through a MATLAB script written to simplify the multidimensional parametric study into a substudy with only two independent variables by selecting values for the remaining parameters. It would then calculate  $P_k$  values for each data point, plot the surface, and perform a quadratic Lowess fit to characterize the resulting graph (as well as possible) mathematically (figure 3). This made trend recognition relatively straightforward and helped choose narrower domains for follow-up analyses. In figure 3, for example, note that  $P_k$  is only weakly dependent on maximum pitch rate of change (*alphadotmax*) but strongly dependent on

maximum thrust rate of change (*ctsigdotmax*). Such dependencies can be explored further by changing the values of the relatively insensitive variable to try to identify an inflection point or by changing the value of a parameter to see if the relationships hold for other related scenarios.

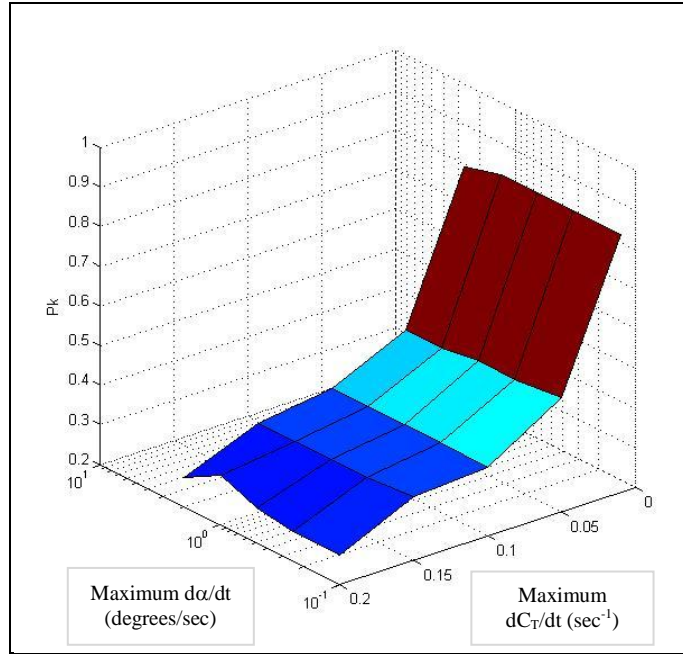


Figure 3.  $P_k$  vs. maximum thrust rate of change (*ctsigdotmax*) and maximum pitch rate of change (*alphadotmax*).

## 2.3 Results

Each of the five studies outlined in section 2.2.3 was performed at least once, and in several cases the analysis domain was repeatedly refined in order to identify variable values of maximum interest. In each study, values not specified by the domain boundaries revert to the default values used for prior analyses of the UH-60. Other vehicles will have different  $P_k$  results, but trends observed within a study should be broadly applicable among vehicles; therefore, the  $P_k$  calculated for a given set of values should be assessed relative to other  $P_k$ 's and not on its absolute value per se, except perhaps as a check for reasonableness. The stress on relative valuations is reinforced in this paper through a consistent axis format and color-mapping schedule for all results presented in this section.

### 2.3.1 Study 1: Gross Weight/Pilot Delay/Velocity Components

The first study compared the effects of changes in gross weight and pilot delay time on  $P_k$ . As seen in figure 4, where  $W_x$  is set to zero, for all values of pilot delay an increase in gross weight is associated with higher  $P_k$ . (This is an intuitive result; a heavier vehicle is more difficult to autorotate.)

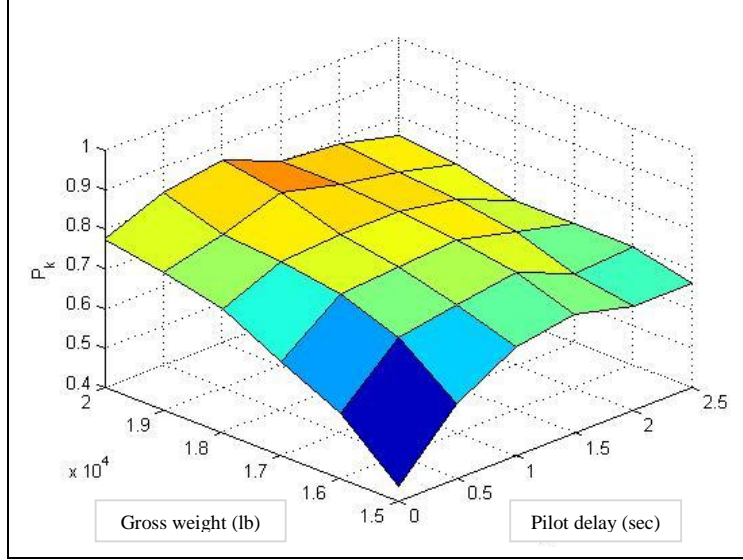


Figure 4.  $P_k$  vs. gross weight and pilot delay for  $W_x = 0$ .

Along the other axis, it is evident that having a minimal pilot delay length is advantageous. However, for values greater than 1 s, that effect dissipates, and in fact the worst  $P_k$  results, dependent on GW, occur in the range of 1–1.5 s of delay.

The same basic trends are evident when  $W_x$  is set to its highest value, 2.0, meaning that impact horizontal velocity is weighted twice as heavily as vertical velocity in the objective function (figure 5). Raising gross weight steadily increases the output  $P_k$ , and the least advantageous values for pilot delay are 1–1.5 s. Note that the entire graph surface is offset higher than in figure 4. This is also an intuitive result since  $P_k$  is based solely on vertical impact velocity: diverting the “attention” of the objective function to a second quantity will reduce its effectiveness in optimizing the original quantity.

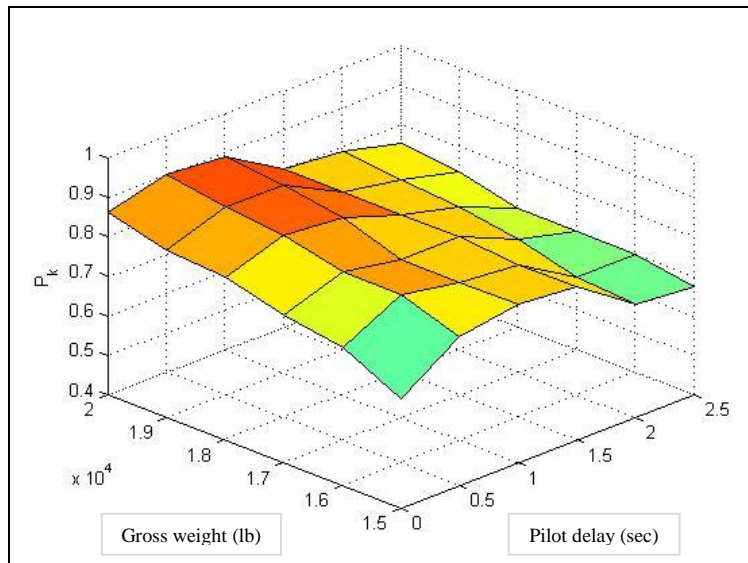


Figure 5.  $P_k$  vs. gross weight and pilot delay for  $W_x = 2.0$ .



This last point is an important insight into the optimization process. The criteria for producing  $P_k$ 's and for selectively optimizing the maneuver within DESCENT may not be well aligned, depending on the prioritization decisions made by the analyst and the physics of the specific scenario under consideration. Kill probability criteria should deal solely with quantities relevant for damage prediction, i.e., impact ratings for structural components or known damage thresholds. DESCENT will encompass these considerations as well as additional limitations on the maneuver, such as a prescribed sink rate during descent or an overemphasis on horizontal speed due to unusual terrain. But it is important for the analyst to understand when, and why, the optimization algorithm's objective function is guiding DESCENT to produce solutions that “score worse” by producing higher  $P_k$ 's.

Using our MATLAB-based visualization script, it was easy to exchange variable axes and show how increasing  $W_x$  affects  $P_k$  for a constant, medium value of gross weight. Figure 6 suggests that  $P_k$  is most sensitive to changes in  $W_x$  in the range  $0 < W_x < 1$  and for low values of pilot delay.

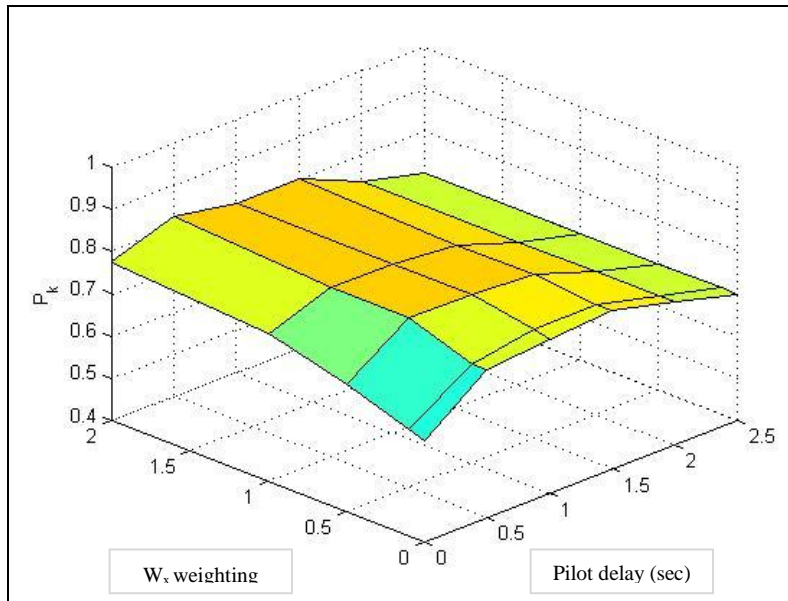


Figure 6.  $P_k$  vs. horizontal velocity weighting and pilot delay for  $GW = 17,000$  lb.

### 2.3.2 Study 2: Fuselage Pitch Target and Weighting

The next study looked at the weighting placed on how closely the fuselage's impact pitch angle matches its target orientation and the setting for that target, against  $W_\theta$  (figure 7). For a given value of  $W_\theta$ , setting a nonzero target pitch orientation almost linearly increases the output  $P_k$  value. The maximum target value,  $\theta_t = 0.4$  rad, corresponds to a nose-up pitch orientation of about  $23^\circ$ , which would be a significant deviation from the pilot's normal objective of a relatively flat, or slightly nose-up, landing.

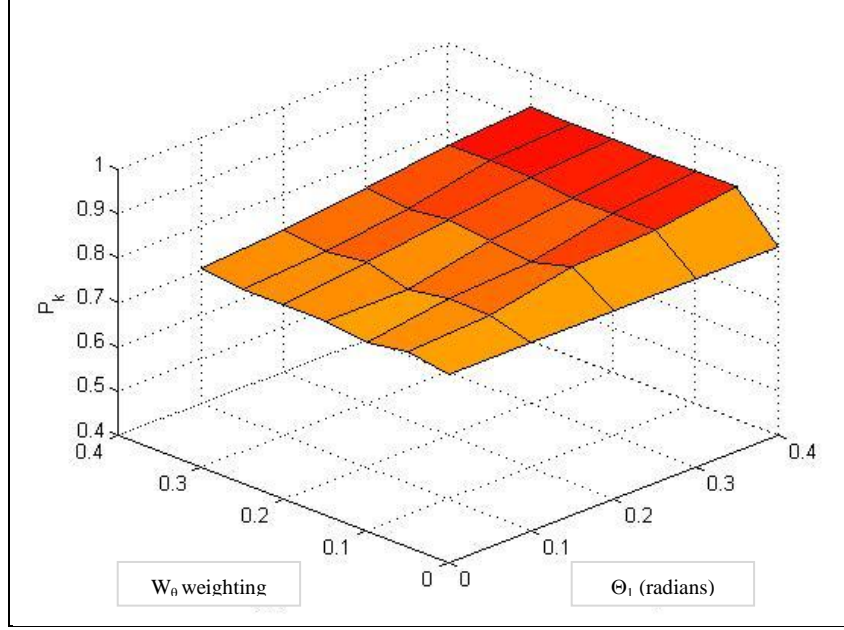


Figure 7.  $P_k$  vs. pitch orientation weighting and target value for  $W_x = 2.0$ .

From a troubleshooting perspective, it is gratifying to see that changes to  $\theta_l$  have no effect for  $W_\theta=0$ , which should be expected since a zero weighting implies that the objective function has no power to enforce whatever target is prescribed in the input file.

This study is most closely aligned with the MADYMO analyses discussed in section 3. If certain impact orientations are found to be most advantageous from an occupant injury perspective, the DESCENT objective function could be changed to encourage that outcome. The question, then, is how much penalty in additional impact velocity is paid for diverting the priorities of the optimization algorithm. Figure 7 appears to show that for reasonable values of target orientation, there is an observable but not prohibitive penalty. Calculating the exact cost/benefit will require additional knowledge of how much the impact velocity is affected at each component and the marginal change in occupant loading for relevant velocity values. Relationships such as those in figure 7 are the first step in the calculation process.

### 2.3.3 Study 3: Max $C_T$ Rate of Change/Max $\alpha$ Rate of Change/Gross Weight

The third study looked at two quantities that DESCENT has traditionally sourced by relatively subjective assumptions to see if more stringent data collection was called for during the analysis process. DESCENT uses two control variables, thrust coefficient ( $C_T$ ), divided by rotor solidity, and rotor-disk angle of attack ( $\alpha$ ), to represent the magnitude and orientation of the thrust vector. These two variables broadly represent the “bottom line” result of whatever the pilot is doing within the two-dimensional plane of motion that DESCENT maneuvers inhabit. Unfortunately,

since neither quantity directly measures a physical control setting (such as stick displacement or throttle setting), finding a reference for quantities like the maximum allowable rate of change of either can be difficult.

Traditionally, DESCENT analyses use the values  $dC_{Tmax} = 0.16$  (in units of one/second) and  $d\alpha_{max} = 0.5$  (in units of degrees/second), which were sourced from subject matter expertise in earlier analyses. Figure 8 plots  $P_k$  against changes in both quantities at the relevant margins for a medium-weight helicopter.

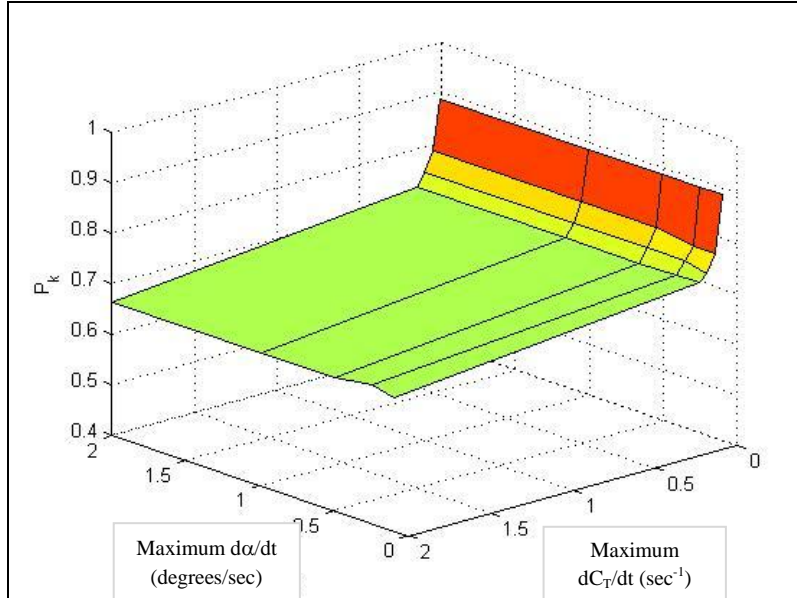


Figure 8.  $P_k$  vs. maximum rates for thrust coefficient and angle of attack.

There is virtually no effect on output by changing  $d\alpha_{max}$ , even to values of 20% of the standard. This insensitivity means that finding more accurate sources for the quantity should be a low priority going forward. On the other axis, it appears that  $dC_{Tmax}$  does have a strong effect on output in the region of the standard value. Although not shown here, the findings are consistent for both higher and lower values of gross weight. One recommendation is that a standard process for calculating a vehicle-specific value for  $dC_{Tmax}$  from vehicle characteristics be developed; this would lend increased confidence to future analyses.

#### 2.3.4 Study 4: In-Maneuver Vertical Speed Weighting and Target/Gross Weight

One aspect of the autorotation maneuver that might be prescribed (for instance, to reflect greater fidelity to flight test data) is the steady rate at which the vehicle descends in the middle part of the maneuver. Study 4 shows that this will be very difficult (figure 9) without more refined targeting of the middle part. As it is, DESCENT's objective function uses an expression for when sinkrate is considered that has a maximum value near the halfway point of the maneuver and zeroes out at the beginning and end, but this is still insufficient to prevent a sink-rate target from interfering with autorotation optimization.

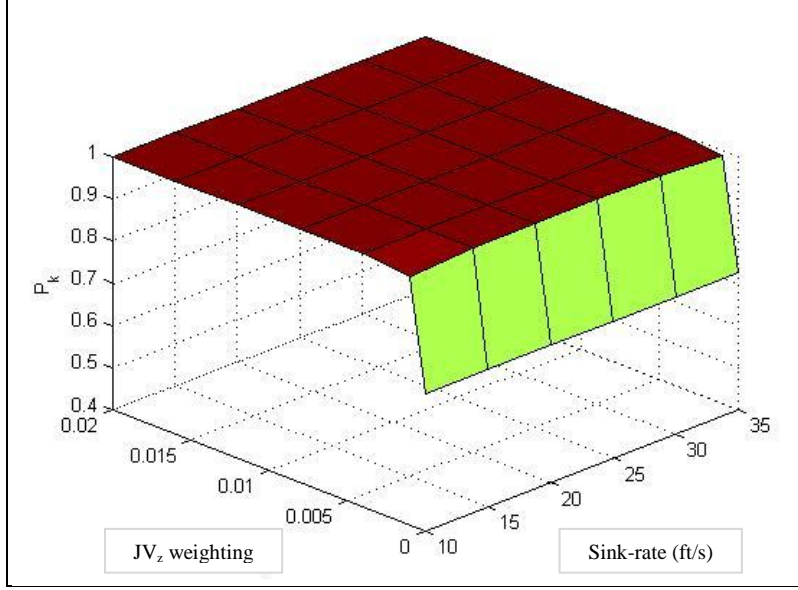


Figure 9.  $P_k$  vs. sink-rate weighting and target value.

Despite several attempts to find lower values for sink-rate weighting ( $J_{V_z}$ ) that might “nudge” the solution without ruining it, there does not appear to be a workable value at this time. As can be seen in figure 9, for any nonzero value of  $J_{V_z}$ ,  $P_k = 1$ , meaning that for any situation in which sinkrate is considered at all, there are no successful autorotations anywhere in the flight envelope. Going forward, a more carefully tailored expression that applies  $J_{V_z}$  during only a narrow portion of the time interval will be required to implement this feature. This will be complicated by the fact that the steady-descent portion of the autorotation encompasses different extents of the autorotation maneuver depending on the initial conditions. A short autorotation from low height may exclude it altogether. So a “test” for steady-state descent might be required instead of a broad expression based on time-wise position within the maneuver.

### 2.3.5 Study 5: Number of Timesteps/Ambient Air Density/Gross Weight

The fifth and final study looked at how the number of discrete time steps used in flight path integration and how the ambient air density affected  $P_k$  output. Air density can be calculated for a desired pressure altitude and air temperature via a standard formula. The density at a pressure altitude of 4000 ft and 95 °F is 0.00193 slug/ft<sup>3</sup>. Our analysis considered densities between 0.0019 and 0.0017 slug/ft<sup>3</sup>, which correspond roughly to pressure altitudes of between 3500 and 7400 ft at 95 °F.

Figure 10 shows the plot of  $P_k$  output for a medium-weight helicopter. There is a strong sensitivity to air density and little to no sensitivity to the number of time steps. Figure 11 shows the same output for a heavier helicopter; the sensitivity to air density has been decreased somewhat, and there is still no sensitivity to changes in the number of time steps employed.

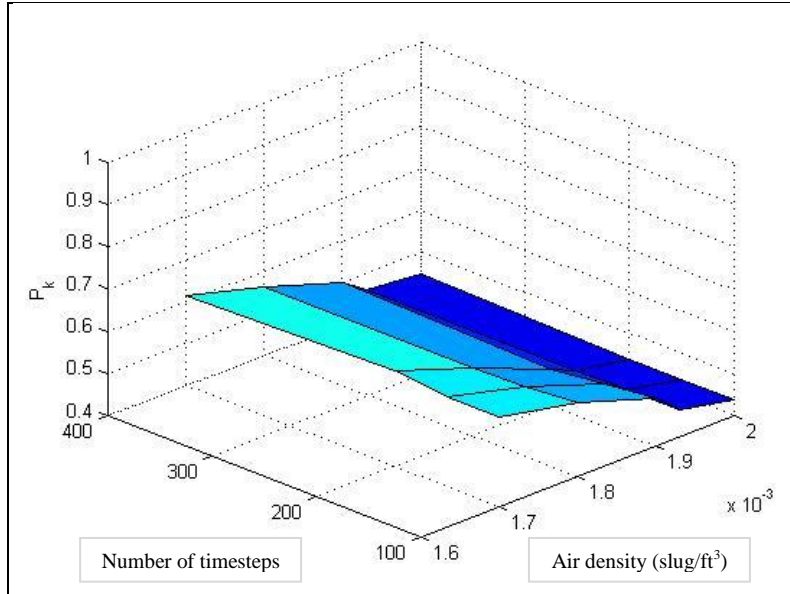


Figure 10.  $P_k$  vs. number of time steps and air density for  $GW = 15,000$  lb.

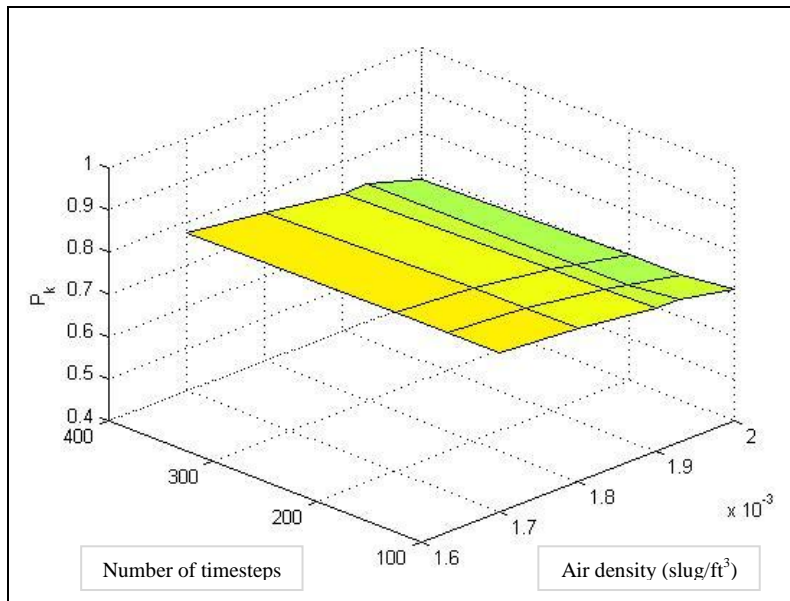


Figure 11.  $P_k$  vs. number of time steps and air density for  $GW = 18,000$  lb.

The first takeaway is that it is very important to be sure of the ambient environment in which the analysis takes place. These conditions will typically be dictated as part of the analysis assignment, but should be double-checked, and it is worth considering the execution of a parallel analysis with slightly less advantageous (higher altitude) conditions to see if the  $P_k$  output is broadly valid for missions occurring in a variety of circumstances.

The second takeaway is that the traditional default setting of  $nt = 200$  is probably far too high. Figure 12 shows that there does not appear to be a marked change in outcome between a lower number of time steps and a higher one—four times as many in this case. To make sure that aggregation of individual outcomes into the  $P_k$  metric did not obscure some underlying sensitivity, the individual case of 100 ft initial height/35 kts initial speed was pulled from the output files for each value of  $nt$ .

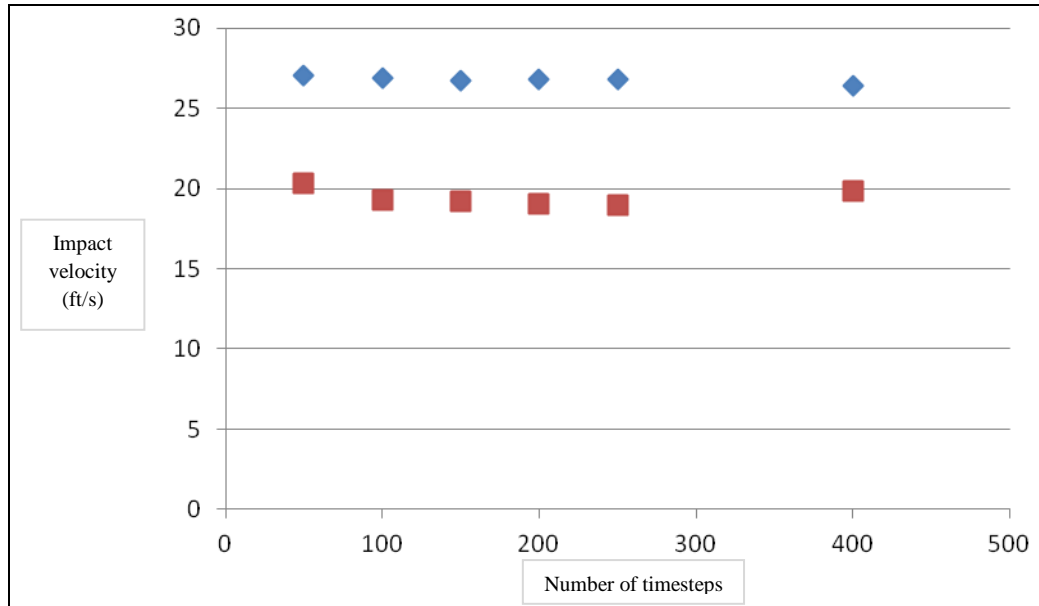


Figure 12. Horizontal (blue) and vertical (red) impact velocities vs. number of time steps.

No significant changes are visible in either horizontal or vertical impact velocities, suggesting similar solutions are reached for each case. Meanwhile, figure 13 shows the additional burden imposed by employing a higher number of time steps. A single execution of DESCENT will take about 5 h at  $nt = 200$ , and there are often upwards of 200 executions in a parametric study such as those discussed here; hence the necessity of the automation (and parallelization) script discussed earlier. But reducing that time to only 20% or so of the normal amount by cutting  $nt$  to about 80 will make parametric studies more feasible and allow them to consider more variables and with more values.

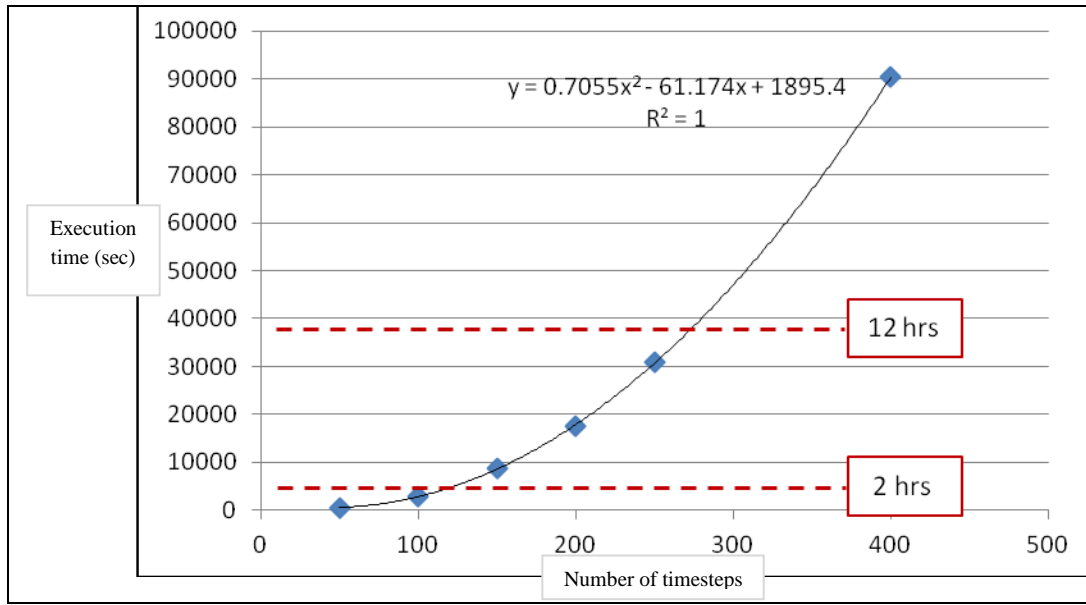


Figure 13. Execution time vs. number of time steps.

### 3. Out-of-Plane Impact Analysis

#### 3.1 Motivation: Intelligent Tradeoffs and Penalties

The motivation behind this portion of the project was to gain insight into how to establish a system of tradeoffs for optimizing impact conditions from an occupant survivability perspective. It is clear from DESCENT work in section 2 that encouraging an arbitrary impact end-state will entail penalties in the form of higher impact velocities (thereby raising loads, possibly increasing vehicle  $P_k$ , and/or injuring occupants). The question, then, is how much is loading reduced by the advantageous end-state, and is the tradeoff worthwhile?

Since the answer to that question is likely to be highly vehicle-specific (as well, possibly, as mission-specific, terrain-specific, and crew-specific), the objective here is simply to work through the process of determining how loading is affected by impact state. From there, decisions can be made about which states must be avoided and which should be encouraged, if the velocity penalties are not prohibitive. This section discusses the structural modeling work and postprocessing done to make some of these observations.

#### 3.2 Description of Work Done

##### 3.2.1 Structural Model Improvement

To capture more applicable data on how impact loads are transferred through a helicopter structure, a considerable effort was expended on upgrading the level of detail and mesh quality of the Bell-206-based helicopter geometry that served as the object of the impact analyses. The



work had three primary goals: improving various aspects of the finite-element mesh on the existing geometry, adding internal structural components that were not modeled originally, and replacing some rigid elements (such as the cockpit face) with realistically characterized deformable elements.

Mesh improvement (figure 14) mainly included reducing the aspect ratio of the individual elements and remeshing certain surfaces to ensure a more consistent element size across components. Additionally, unusually shaped elements (triangles or distorted quadrilaterals) were replaced by more regular quadrilaterals where possible. These improvements helped increase the efficiency and accuracy of the finite-element analysis (FEA) modeling.

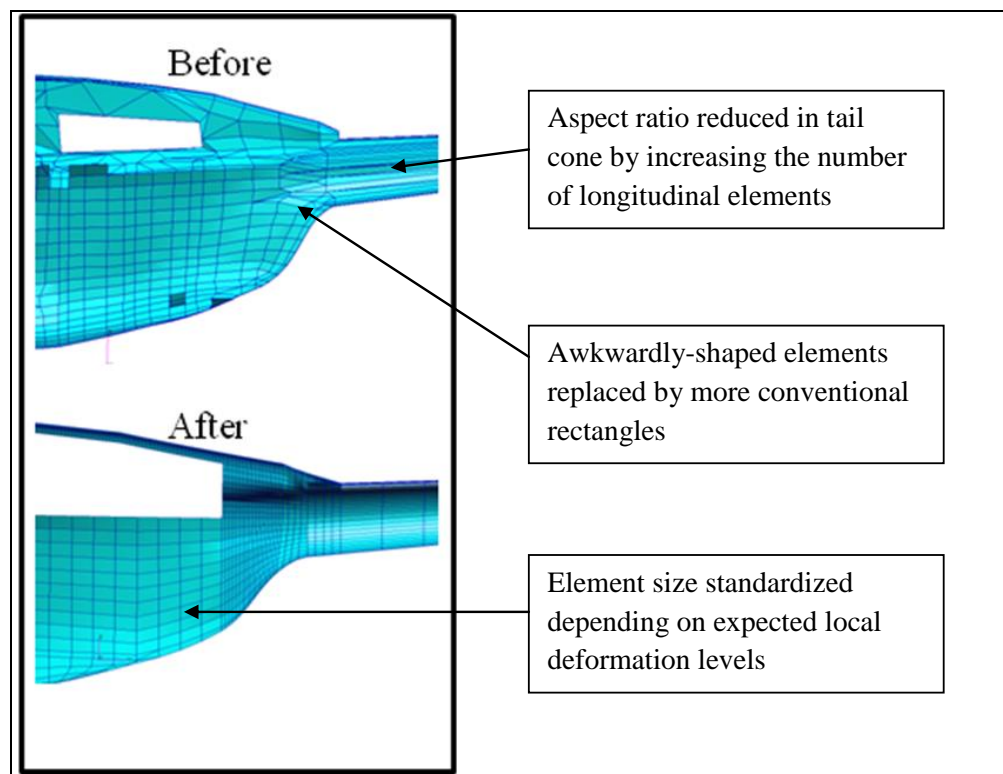


Figure 14. Example of mesh improvement in Bell-206-based structural model.

### 3.2.2 Pitch and Roll Study

The improved helicopter model was then used to perform a series of ground-surface impacts for the study of how fuselage impact orientation affected occupant loading. This study, which was done with the MADYMO structural dynamics FEA program, involved modeling impacts at various fuselage orientations of pitch and roll, as well as several velocity vectors and magnitudes. Output consisted of time histories of loading levels on the pilot and copilot “dummies” in the model. Figure 15 shows a screenshot from the impact event and a trace of the copilot’s neck moment for a hard vertical impact with strong nose-down and rolled fuselage orientations (figure 16), a nearly worst-case scenario.





Figure 15. Helicopter model impacting vertically at 10° (nose-down) pitch and 10° (port) roll.

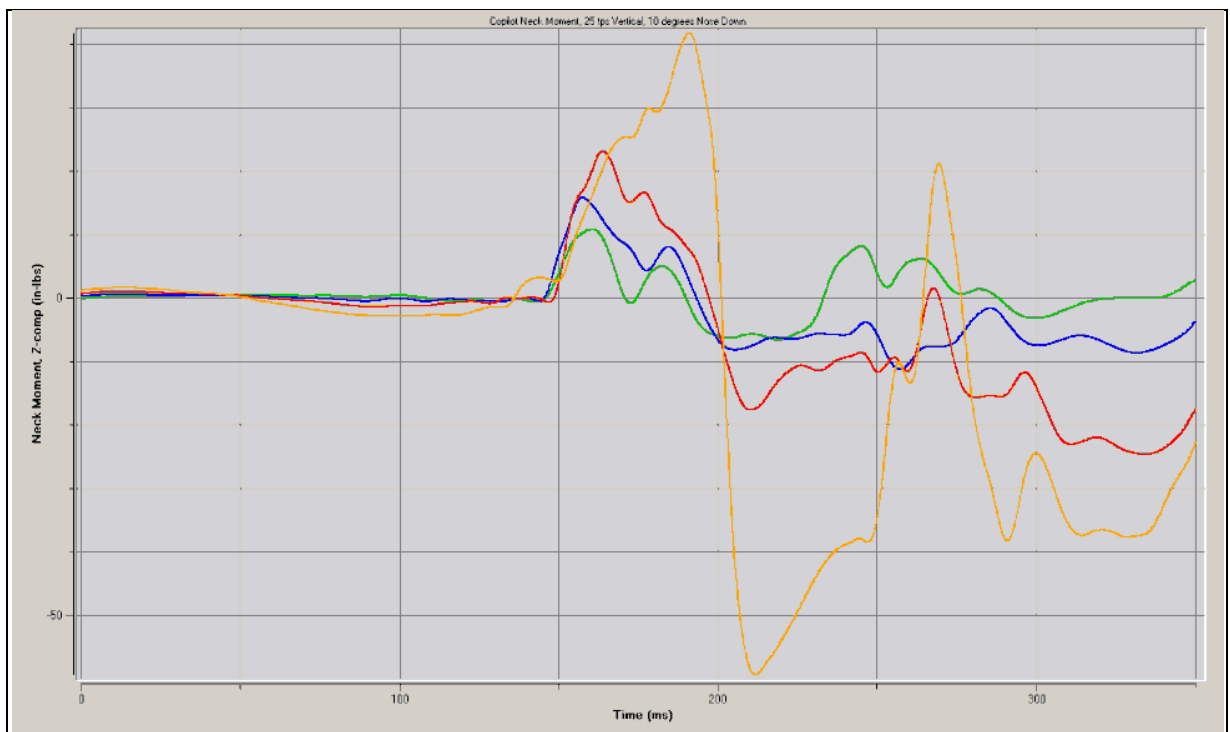


Figure 16. Copilot neck moments for 10° (nose-down) pitch impacts. Roll conditions are flat (green), 2° (blue), 5° (red), and 10° (yellow).

### 3.3 Results

The MADYMO study modeled three loading conditions: neck torque, pelvic acceleration, and lumbar loading, in all three local coordinate axes. These loads were modeled for two crew member sizes, the 95th-percentile pilot and 50th-percentile copilot.

For conditions at time of impact, the following test matrix was executed:

- Two velocities: 25 ft/s pure vertical; and 25 ft/s vertical, 25 ft/s horizontal.
- Three pitch angles: 0° (flat), 10° (nose up), and –10° (nose down).
- Four roll angles: 0°, 2°, 5°, and 10°.

This comprises 24 executions at 18 loading time histories per execution. Selected results are presented for both the time histories within a single pitch condition, as in figure 16, and for peak loading conditions across pitch conditions.

### 3.3.1 Loading Time Histories

All loads are decomposed into x-, y-, and z-axis components in the local (sensor-centered) coordinate system. Since the coordinate system is attached to the “sensor,” in most cases an increase in roll orientation leads to a slight decrease in z-axis loading and a significant increase in y-axis loading, simply because the impact vector is no longer aligned with the sensor axes (figures 17 and 18). Calculation of the compound (triaxial) loading magnitudes is scheduled for 2014, but since in many cases the injury criteria is expressed in terms of unidirectional loads in the local reference frame, these results are relevant to occupant injury prediction.

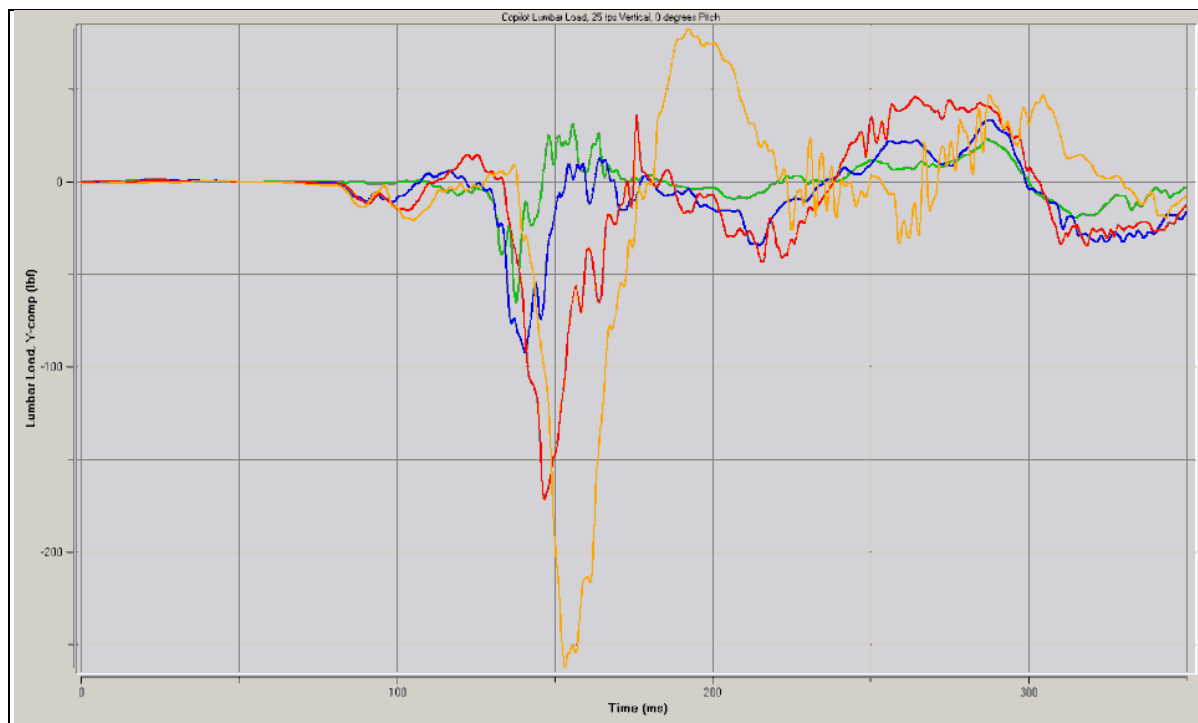


Figure 17. Copilot y-axis lumbar loads for vertical impact and flat landing. In each figure, green, blue, red, and yellow traces represent 0°, 2°, 5°, and 10° of fuselage roll, respectively.

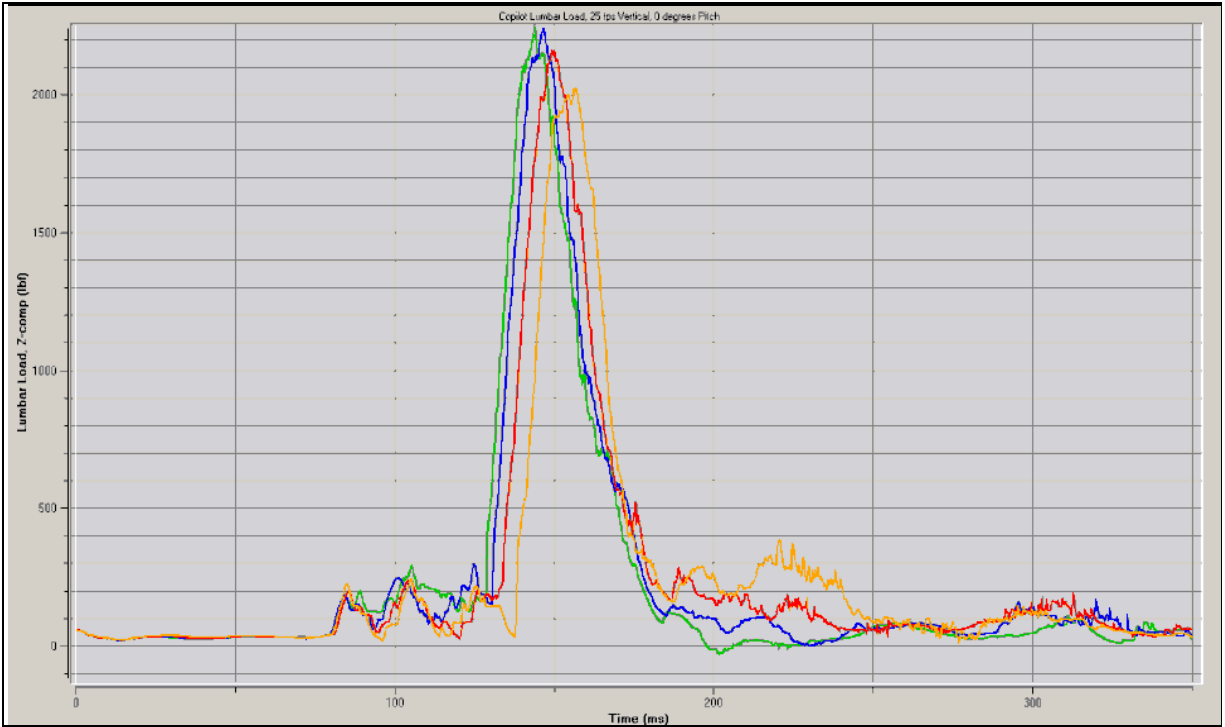


Figure 18. Copilot z-axis lumbar loads for vertical impact and flat landing.

It can be seen from the previous figures that for all roll orientations, z-axis (vertical) loading predominates, accounting for up to about 90% of the total loading. It is also apparent that increasing the fuselage roll angle induces a slight delay in the response curve; this is a consistent feature of the results that is unexplained at this time.

The shape of the z-axis lumbar loading curve is mostly independent of pitch state, but x- and y-axis curves vary significantly between nose-up and nose-down impacts. Figure 19 shows the nose-up time histories; x-loading peaks at about 300 lb and is mostly independent of roll state, whereas y-loading is less than 100 lb and subject to much more noise.

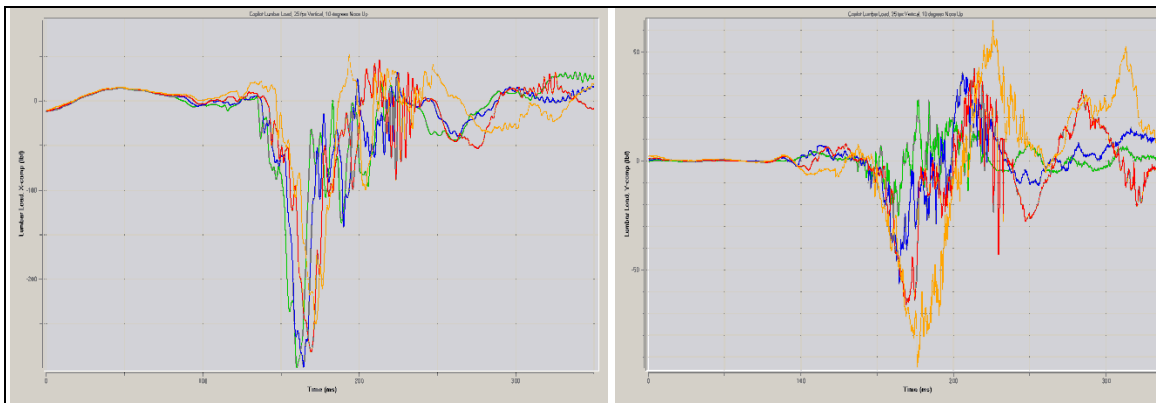


Figure 19. Copilot x-axis (left) and y-axis (right) lumbar loads for vertical impact and nose-up landing.

Figure 20 shows the same quantities during a nose-down impact. While the y-axis plot shows the same roll sensitivity, noisy trends, and relatively low peak magnitude as in the nose-up case, the x-axis plot is altogether different. There are two distinct loading peaks of nearly equal magnitude for every roll level, and a large segment of negative loading between. In addition, the peak magnitudes are significantly lower than in the nose-up case, which contradicts some intuitive thinking about piloting strategies.

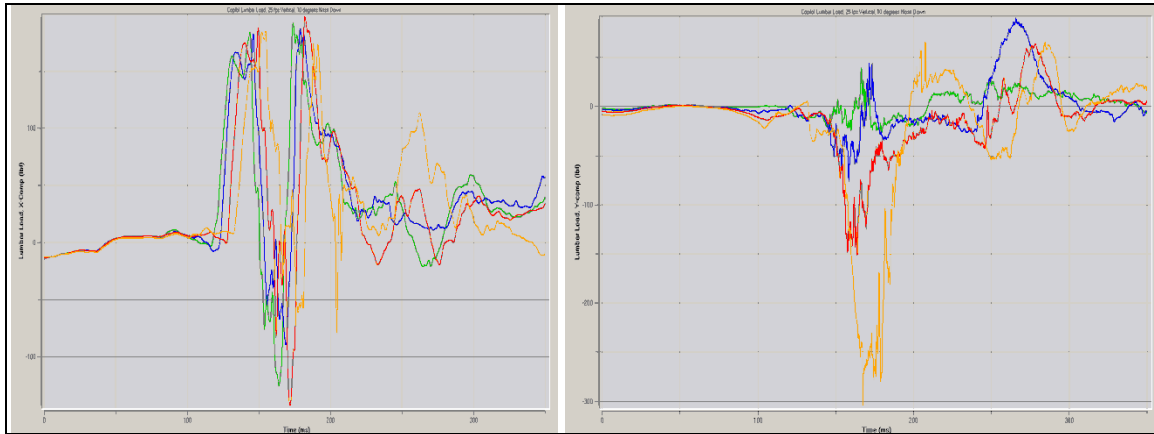


Figure 20. Copilot x-axis (left) and y-axis (right) lumbar loads for vertical impact and nose-down landing.

Occasionally, roll would appear to be an insignificant factor until a threshold level was reached. Figure 21 shows pilot x- and z-axis neck moments. Peak magnitude is small and barely increases with roll until the last data series, wherein a  $10^\circ$  roll state induces a moment three to four times greater than the next highest case. As more of these cases are identified, they can be coded into DESCENT as outcomes to avoid by making the objective function penalty highly nonlinear as the thresholds are approached. This will assist in finding only solutions that steer clear of dangerous impact states for the occupants.

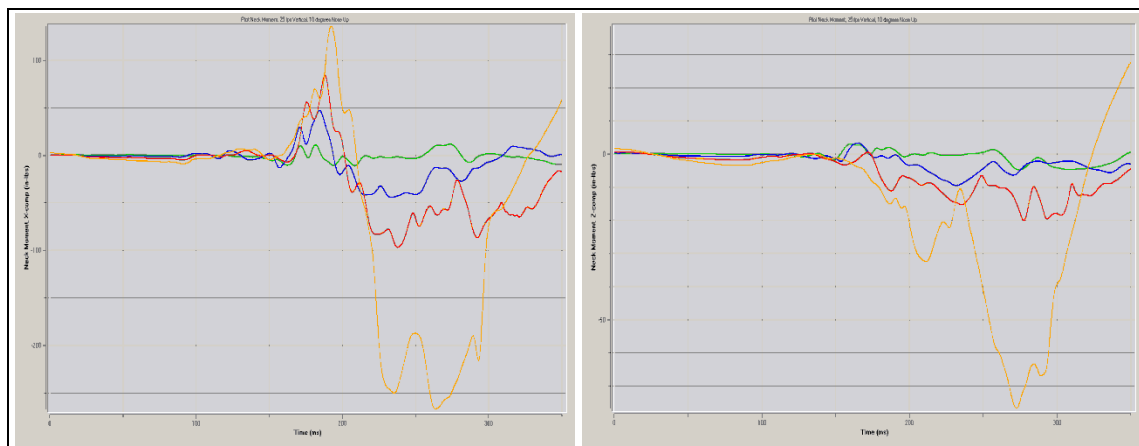


Figure 21. Pilot x-axis (left) and z-axis (right) neck moments for vertical impact and nose-up landing.

The full set of time history plots was produced by the U.S. Naval Air Systems Command in an unpublished white paper and is available from the author upon request, subject to release restrictions.

### 3.3.2 Peak Magnitudes

Since many injury criteria are in terms of peak magnitude, loading rate data can often be excluded and time histories condensed to simply plots of peak loading magnitudes. This helps to visualize trends in the severity of loading as a function of impact state. Using a MATLAB script to visualize the data, several trends were evident and are described in the following.

Figure 22 typifies the observation that in many cases, especially for z-axis loading, the flat landing was the most severe. This is strong motivation for additional consideration in the DESCENT objective function of a nonzero impact fuselage pitch. Interestingly, the figure also shows that the severity of the flat landing decreases with roll angle, meaning that the “perfect” landing is the least optimal in the case of minimizing pelvic acceleration.

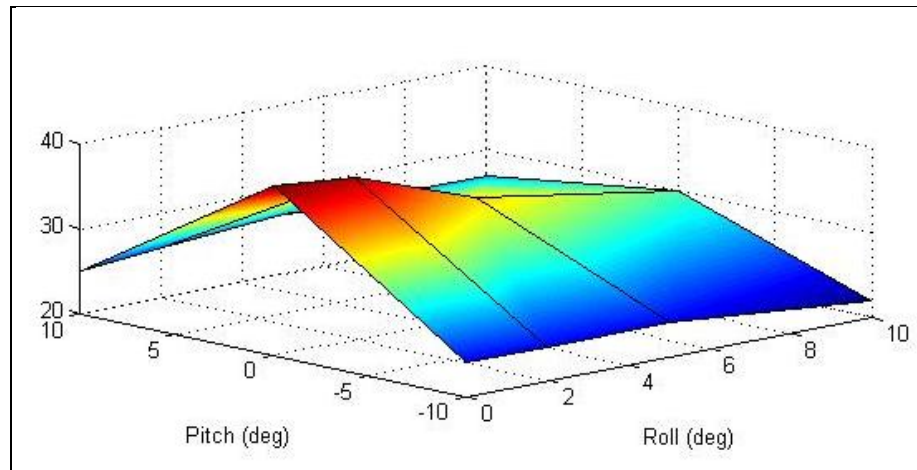


Figure 22. Pilot z-axis pelvic acceleration (g) vs. pitch and roll impact state.

For y-axis loading, trends discussed in section 2 are increasingly clear. Figure 23 shows that peak pelvic acceleration is four to five times higher under a condition of high roll than under a flat landing. Furthermore, the peak magnitude jumps quickly at the higher roll angles, suggesting a threshold of nonlinearity. At higher roll angles, the flat landing is once again least optimal, although the nose-up landing is least optimal for lower roll angles.

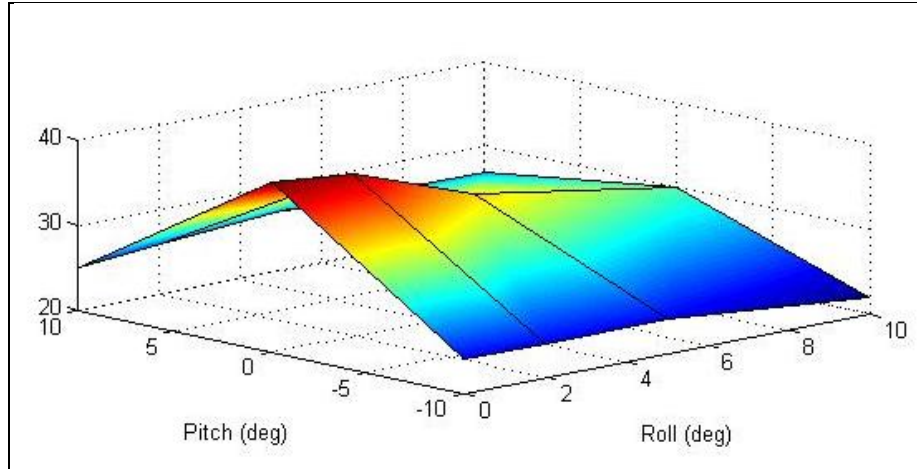


Figure 23. Pilot z-axis pelvic acceleration (g) vs. pitch and roll impact state.

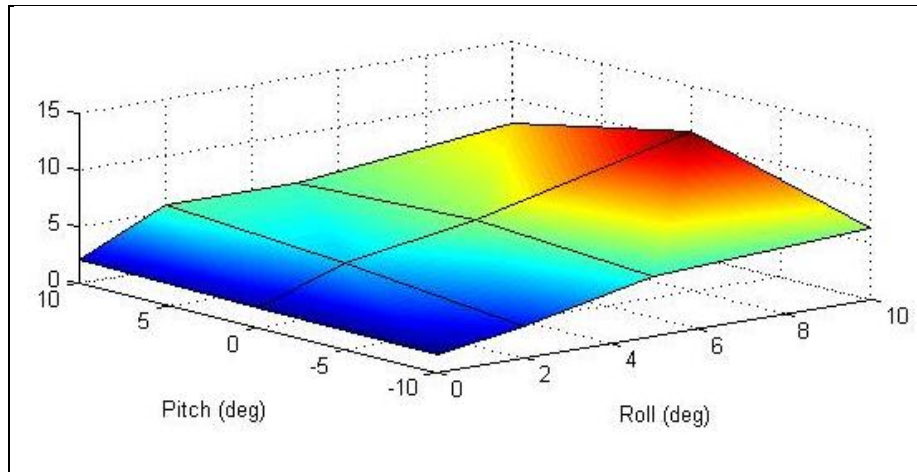


Figure 24. Pilot y-axis pelvic acceleration (g) vs. pitch and roll impact state.

One additional observation is that an asymmetry exists between the copilot and pilot loading experiences. For the case shown in figure 23, y-axis pelvic acceleration, the copilot experienced loads averaging 15% higher than the pilot, although not uniformly higher. It is unclear whether this discrepancy is due to the sizes of the modeled occupants (the pilot is 90th percentile and the copilot is 50th percentile) or due to the fact that roll was modeled only to one side (meaning that the occupants experienced slightly different load-transfer environments). Either way, this should be accounted for in a fully mature occupant injury model. Position and size appear to have noticeable effects on loading, so predictions should be valid for all relevant occupant positions and a broad range of sizes.

---

## 4. Conclusions

---

The parametric autorotation study portion of this project was able to successfully demonstrate how different piloting strategies in the DESCENT model, as well as various other parameter values, affect the optimality of the eventual solution. Specifically, it was shown that vehicle weight has a consistent, nearly linear relationship to  $P_k$ . The effect of pilot delay is more complicated, as values in the neighborhood of 1 s appear to be least optimal for reasons not fully understood. Parameters such as maximum pitch rate and number of time steps appear to have little influence on solutions, at least at relevant values. Increased emphases on both horizontal impact speed and fuselage impact pitch orientation appear to have mildly negative effects on vertical impact speed. Finally,  $P_k$  is strongly sensitive to ambient air density and how quickly the rotor's thrust level is allowed to change, and there appears to be no "safe" way to influence the algorithm toward a desired sink-rate without sacrificing overall successfulness. These lessons will guide future development of the DESCENT code and inform both data gathering and mission definition for future analyses.

The MADYMO-supported portion of this project also facilitated several lessons learned with respect to encouraging optimal landing conditions for occupants. It is not known without further study to what extent these are general truisms, or to what extent they only apply to Bell-206 versions, but it seems intuitive that they should be broadly applicable. First, increased fuselage roll predictably decreases occupant loading in the local z-axis and increases it significantly in the local y-axis. Second, even in cases where small levels of roll have linear relationships to loading experiences, there can be cutoff thresholds above which loading increases substantially. Third, moderate pitch states yield unpredictable and seemingly inconsistent effects on loading in all axes. Fourth, the flat landing is often nonoptimal from a loading perspective.

The global conclusion from the MADYMO study is that different loading modes are affected by impact state in different ways. This is important because it means that not only must tradeoffs be designed between impact velocity and impact state, but also between various injury modes. In other words, a set of DESCENT objective function parameter values designed to produce an impact state that minimizes pelvic acceleration might easily produce nonoptimal levels of neck loading or lumbar loading. So the tradeoffs must be managed iteratively and interactively.

It is recommended that a flexible procedure for characterizing those tradeoffs and relating them to each other is designed and implemented with the existing structural dynamics model and a modified version of the DESCENT code. Demonstration of an autorotation optimization that has an integrated capability of mitigating occupant loading would be an important step forward in advancing occupant-focused survivability/vulnerability analyses.

NO. OF  
COPIES ORGANIZATION

1 (PDF)	DEFENSE TECHNICAL INFORMATION CTR DTIC OCA
1 (PDF)	DIRECTOR US ARMY RESEARCH LAB IMAL HRA
1 (PDF)	DIRECTOR US ARMY RESEARCH LAB RDRL CIO LL
1 (PDF)	GOVT PRINTG OFC A MALHOTRA
1 (PDF)	USARL RDRL SLE R FLORES
1 (HC)	DIR US ARMY EVALUATION CTR HQ TEAE SV P A THOMPSON 2202 ABERDEEN BLVD 2ND FL APG MD 21005-5001
4 (2 HC 2 PDF)	DIR USARL RDRL SL J BEILFUSS P TANENBAUM RDRL SLB A M PERRY (PDF only) RDRL SLB D A DRYSDALE